Journal of Pharmacology and Toxicology

ISSN 1816-496X

Academic Journals Inc.

www.academicjournals.com

Journal of Pharmacology and Toxicology 3 (1): 11-19, 2008
ISSN 1816-496X

Molecular Modelling Analysis of the Metabolism of Methimazole

Fazlul Huq
Discipline of Biomedical Science, School of Medical Sciences, Faculty of Medicine, Cumberland Campus, C42, University of Sydney, Lidcombe, NSW, Australia

Abstract: Molecular modelling analyses based on molecular mechanics, semi-empirical (PM3) and DFT (at B3LYP/6-31G* level) calculations show that MET and its major metabolites have LUMO-HOMO energy differences ranging from 4.1 to 6.7 eV from DFT calculations, indicating that they would vary significantly in their kinetic inertness. The molecular surfaces of MET, MTU, MET-EPO and GLX are found to possess significant amounts of electron-deficient regions so that they can react with cellular nucleophiles such as glutathione and nucleobases in DNA, thus causing depletion of glutathione and oxidation of nucleobases. The former would induce cellular toxicity due to oxidative stress and the latter would cause DNA damage. The rates of such adverse reactions are expected to be significant for GLX which would be moderately labile kinetically. This means that the toxicity due to MET may be mediated via the formation of GLX although the parent drug itself may also be responsible for toxicity if the rates of its reactions with glutathione and nucleobases in DNA are speeded up enzymatically.

Key words: Methimazole, auto-immune disease, anti-inflammatory agent, glutathione, hepatotoxicity, molecular modelling

INTRODUCTION

Methimazole (2-mercapto-1-methylimidazole, MET) is a tautomeric cyclic thione used to treat various auto-immune diseases such as hyperthyroidism in humans (Meng, 2006). MET represses the thyroid function through irreversible inhibition of the thyroid peroxidase needed for the synthesis of thyroid hormones (Engler *et al*., 1982). MET could also act as an anti-inflammatory agent through inhibition of adhesion molecules. However, MET therapy in humans is found to be associated with a number of adverse effects including agranulocytes, immunologic disturbances, bone marrow depression and liver damage (Schimdt *et al*., 1986; Vitug and Goldman, 1985; Wing and Fantus, 1987). Also, the drug is reported to affect the sense of smell and taste (Schiffman, 1983). MET induces severe hepatotoxicity in mice that have been depleted of glutathione (GSH) by pre-treatment with DL-Buthionine Sulf Oxine (BSO), in inhibitor of GSH synthesis (Mizutani *et al*., 1999).

MET is metabolized to produce a number of metabolites including 2-mercaptoimidazole (SHMET), N-Methyl Thio Urea (MTU) and 1-Methyl Hydantoin (MEH). It has been suggested that toxicity of MET is due to its molecular activation. First MET is believed to be oxidized to form methimazole-4,5-epoxide (MET-EPO) (catalyzed by cytochrome P450 oxidases) which is then aquated to form unstable intermediate methimazole-4,5-diol (MET-DIOL). MET-DIOL spontaneously breaks down to form Glyoxal (GLX) and N-Methyl Thio Urea (MTU). MTU is further oxidized to its S-oxidized metabolites MTU-sulhydroxyl (MTUOH) and MTU-sulf-oxo-hydroxyl (MTUO2H). MTUOH and MTUO2H are believed to be responsible for hepatotoxicity of MET (Mizutani *et al*. 1999).

In this study, molecular modelling analyses have been carried out using the program Spartan '02 (Spartan, 2002) to investigate the relative stability of MET and its metabolites with the aim of

providing a better understanding on their relative toxicity. The study done in the Discipline of Biomedical Science, School of Medical Sciences, The University of Sydney during January to February 2007.

COMPUTATIONAL METHODS

The geometries of MET and its metabolites (Fig. 1) have been optimized based on molecular mechanics, semi-empirical and Density Functional Theory (DFT) calculations, using the molecular modelling program Spartan '04. Molecular mechanics calculations were carried out using MMFF force field. Semi-empirical calculations were carried out using the routine PM3. DFT calculations were carried at B3LYP/6-31G* level. In optimization calculations, a RMS gradient of 0.001 was set as the terminating condition. For the optimized structures, single point calculations were carried out to give heat of formation, enthalpy, entropy, free energy, dipole moment, solvation energy, energies for Highest Occupied Molecular Orbit HOMO and Lowest Unoccupied Molecular Orbit LUMO. The order of calculations: molecular mechanics followed by semi-empirical followed by DFT ensured that the structure was not embedded in a local minimum. To further check whether the global minimum was reached, some calculations were carried out with improvable structures. It was found that when the stated order was followed, structure corresponding to the global minimum or close to that could

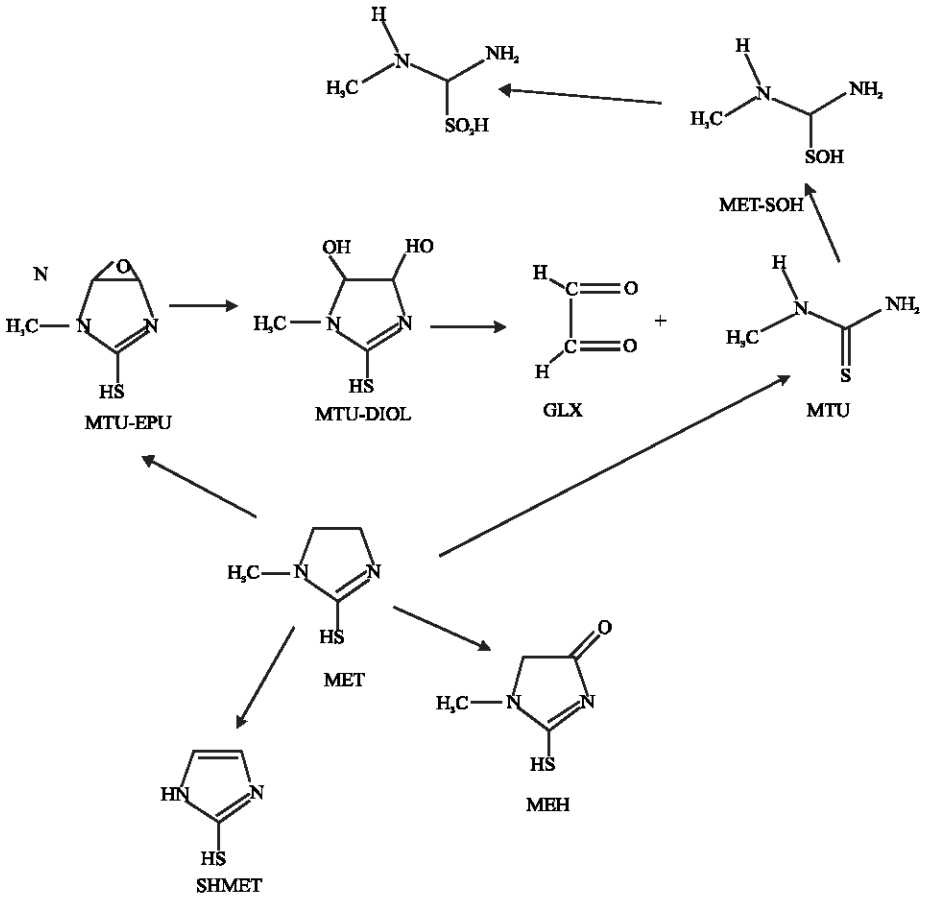

Fig. 1: Metabolic pathway for MTU

ultimately be reached in all cases. Although RMS gradient of 0.001 may not be sufficiently low for vibrational analysis, it is believed to be sufficient for calculations associated with electronic energy levels.

RESULTS AND DISCUSSION

Table 1 gives the total energy, heat of formation as per PM3 calculation, enthalpy, entropy, free energy, surface area, volume, dipole moment and energies of HOMO and LUMO as per both PM3 and DFT calculations for MET and its metabolites SHMET, MTU, MEH, MET-EPO, MTU-DIOL, GLX, MTU-OH and MTUO2H. Figure 2-10 give the regions of negative electrostatic potential (greyish-white envelopes) in (a), HOMOs (where red indicates HOMOs with high electron density) in (b), LUMOs in © and density of electrostatic potential on the molecular surface (where red indicates negative, blue indicates positive and green indicates neutral) in (d) as applied to optimized structures of MET and its metabolites SHMET, MTU, MEH, MET-EPO, MTU-DIOL, GLX, MTU-OH and MTUO2H.

Table 1: Calculated thermodynamic and other parameters of MET and its metabolites

Molecule	Calculation type	Total energy (kcal mol^{-1} / atomic unit*)	Heat of formation (kcal mol^{-1})	Enthalpy (cal mol^{-1})	Entropy (cal mol^{-1} K^{-1})	Free energy (kcal mol^{-1})	Solvation energy (kcal mol^{-1})
MET	PM3	26.04	32.99	63.27	83.91	38.25	-6.95
	DFT	-663.71		66.36	84.09	41.29	-8.26
SHMET	PM3	21.94	33.55	45.42	75.66	22.86	-11.61
	DFT	-62.41		47.58	76.98	24.63	-11.64
MTU	PM3	6.84	23.69	58.01	77.76	34.83	-16.85
	DFT	-587.53		60.32	78.75	36.84	-15.55
MEH	PM3	-88.50	-79.01	68.80	81.63	44.46	-9.49
	DFT	-416.02		73.12	85.20	47.20	-7.86
MET-EPO	PM3	11.83	27.75	65.95	86.12	40.28	-15.92
	DFT	-738.89		69.40	86.37	43.64	-16.48
MTU-DIOL	PM3	-77.81	-67.49	84.71	95.07	56.37	-10.31
	DFT	-815.35		88.24	97.14	59.28	-10.27
GLX	PM3	-70.30	-62.26	25.23	63.70	6.24	-8.04
	DFT	-227.81		25.85	66.68	5.97	-6.39
MTU-OH	PM3	-36.84	-49.33	75.86	88.77	49.39	-12.49
	DFT	-663.89		77.85	86.62	52.03	-14.72
MTU-O2H	PM3	-94.50	-76.77	78.50	94.32	50.38	-17.72
	DFT	-739.09		80.71	91.80	53.34	-17.30

Molecule	Calculation type	Solvation energy (kcal mol^{-1})	Area (Å 2)	Volume (Å 3)	Dipole moment (debye)	HOMO (eV)	LUMO (eV)	LUMO-HOMO (eV)
MET	PM3	-6.95	136.52	112.54	2.9	-8.72	-0.17	8.55
	DFT	-8.26	134.96	111.56	3.0	-5.60	0.34	5.94
SHMET	PM3	-11.61	115.33	92.11	2.5	-8.97	-0.25	8.72
	DFT	-11.64	114.64	91.49	2.6	-5.72	0.16	5.88
MTU	PM3	-16.85	114.52	87.14	6.0	-8.72	-0.66	8.06
	DFT	-15.55	114.01	86.8	5.8	-5.42	0.15	5.57
MEH	PM3	-9.49	133.93	109.31	2.7	-9.79	0.27	10.06
	DFT	-7.86	132.17	108.12	2.6	-6.98	-0.32	6.66
MET-EPO	PM3	-15.92	141.72	118.37	1.6	-9.54	-0.50	9.04
	DFT	-16.48	140.07	116.93	2.8	-6.47	0.06	6.53
MTU-DIOL	PM3	-10.31	156.31	130.84	0.9	-9.44	-0.50	8.94
	DFT	-10.27	155.17	129.97	1.3	-6.24	0.16	6.40
GLX	PM3	-8.04	78.91	57.50	3.4	-10.43	-0.55	9.88
	DFT	-6.39	79.26	57.77	3.3	-7.26	-3.13	4.13
MTU-OH	PM3	-12.49	135.69	102.23	2.2	-9.24	-0.02	9.22
	DFT	-14.72	134.89	101.82	2.2	-5.91	-0.22	5.69
MTU-O2H	PM3	-17.72	145.78	110.23	1.6	-9.95	-0.12	9.83
	DFT	-17.30	141.17	109.40	3.0	-5.83	-0.10	5.73

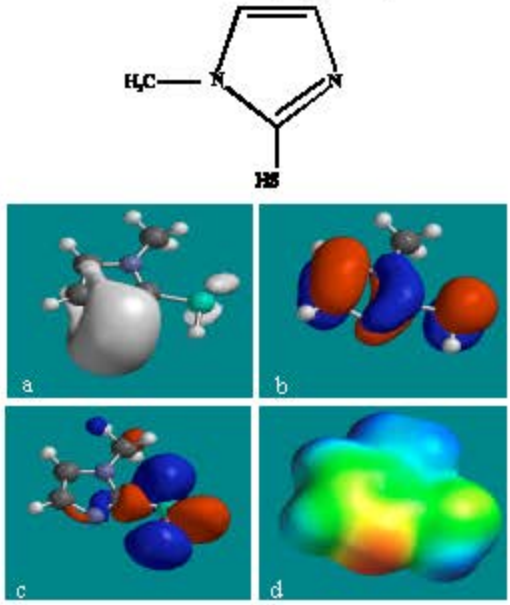

Fig. 2: Structure of MET giving in: (a) the electrostatic potential (greyish envelope denotes negative electrostatic potential), (b) the HOMOs, (where red indicates HOMOs with high electron density) (c) the LUMOs (where blue indicates LUMOs) and in (d) density of electrostatic potential on the molecular surface (where red indicates negative, blue indicates positive and green indicates neutral)

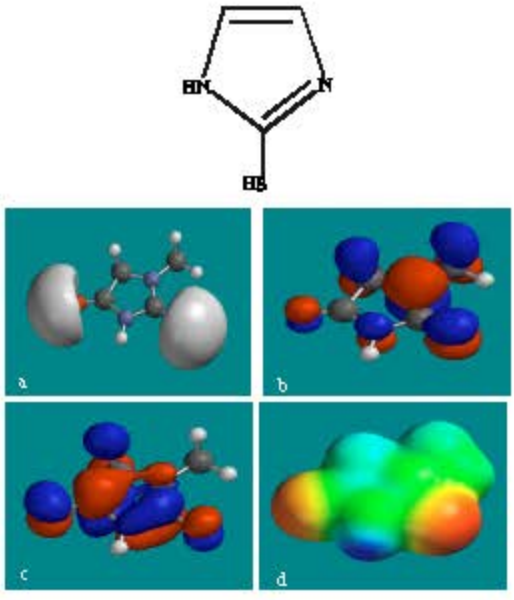

Fig. 3: Structure of SHMET giving in: (a) the electrostatic potential (greyish envelope denotes negative electrostatic potential), (b) the HOMOs, (where red indicates HOMOs with high electron density) (c) the LUMOs (where blue indicates LUMOs) and in (d) density of electrostatic potential on the molecular surface (where red indicates negative, blue indicates positive and green indicates neutral)

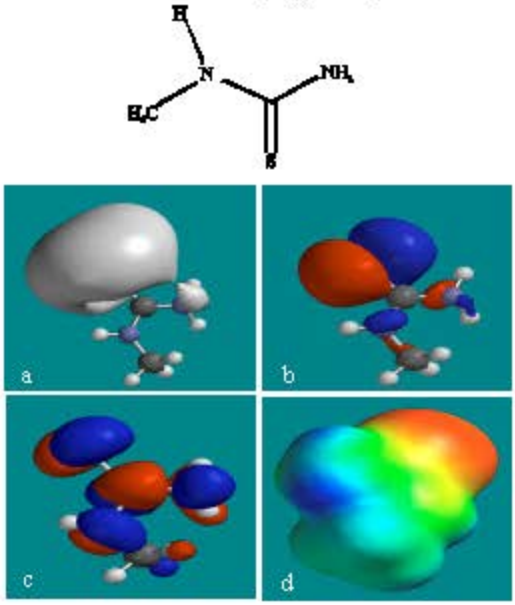

Fig. 4: Structure of MTU giving in: (a) the electrostatic potential (greyish envelope denotes negative electrostatic potential), (b) the HOMOs, (where red indicates HOMOs with high electron density) (c) the LUMOs (where blue indicates LUMOs) and in (d) density of electrostatic potential on the molecular surface (where red indicates negative, blue indicates positive and green indicates neutral)

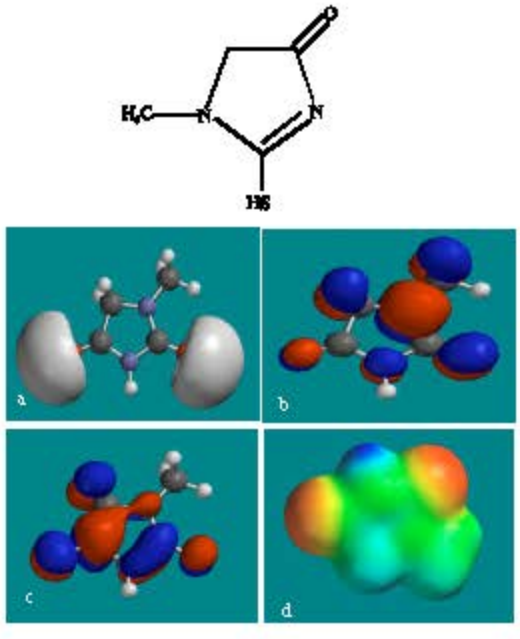

Fig. 5: Structure of MEH giving in: (a) the electrostatic potential (greyish envelope denotes negative electrostatic potential), (b) the HOMOs, (where red indicates HOMOs with high electron density) (c) the LUMOs (where blue indicates LUMOs) and in (d) density of electrostatic potential on the molecular surface (where red indicates negative, blue indicates positive and green indicates neutral)

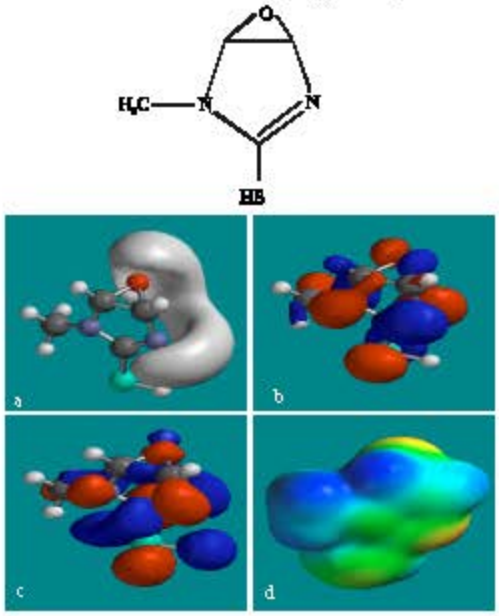

Fig. 6: Structure of MET-EPO giving in: (a) the electrostatic potential (greyish envelope denotes negative electrostatic potential), (b) the HOMOs, (where red indicates HOMOs with high electron density) (c) the LUMOs (where blue indicates LUMOs) and in (d) density of electrostatic potential on the molecular surface (where red indicates negative, blue indicates positive and green indicates neutral)

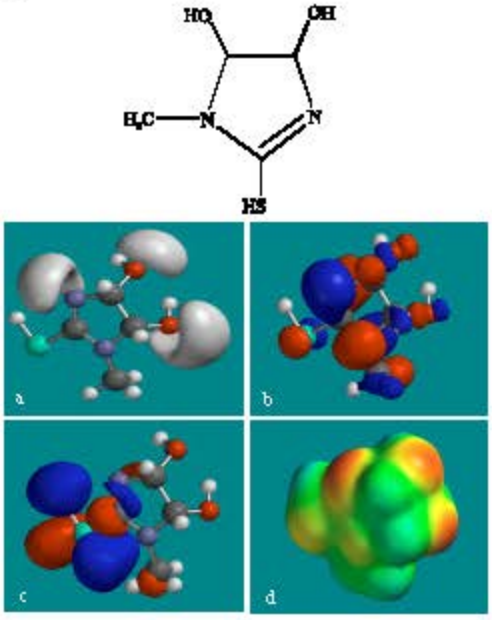

Fig. 7: Structure of MET-DIOL giving in: (a) the electrostatic potential (greyish envelope denotes negative electrostatic potential), (b) the HOMOs, (where red indicates HOMOs with high electron density) (c) the LUMOs (where blue indicates LUMOs) and in (d) density of electrostatic potential on the molecular surface (where red indicates negative, blue indicates positive and green indicates neutral)

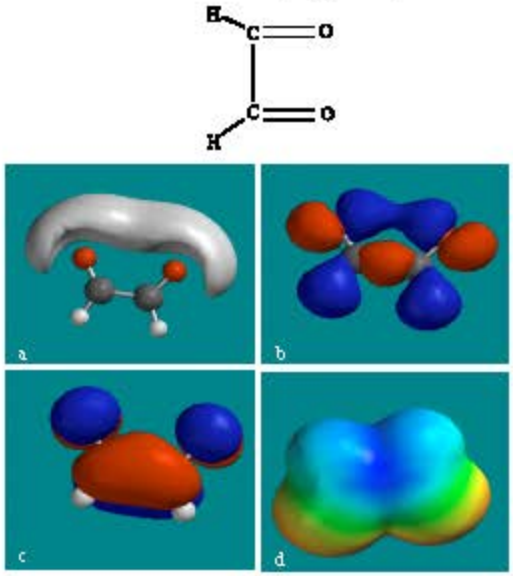

Fig. 8: Structure of GLX giving in: (a) the electrostatic potential (greyish envelope denotes negative electrostatic potential), (b) the HOMOs, (where red indicates HOMOs with high electron density) (c) the LUMOs (where blue indicates LUMOs) and in (d) density of electrostatic potential on the molecular surface (where red indicates negative, blue indicates positive and green indicates neutral)

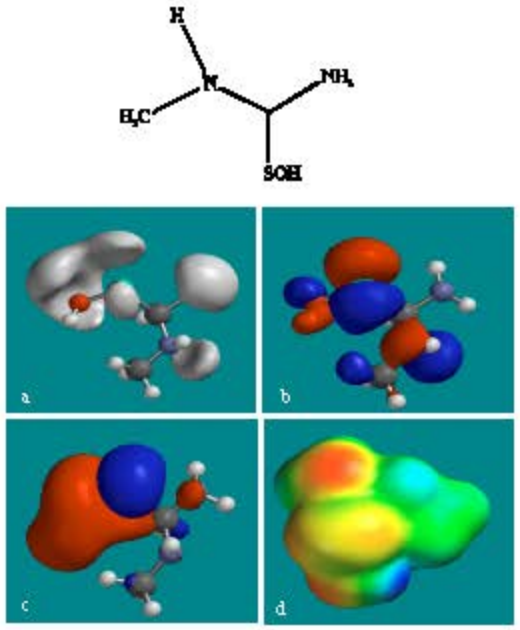

Fig. 9: Structure of MTU-OH giving in: (a) the electrostatic potential (greyish envelope denotes negative electrostatic potential), (b) the HOMOs, (where red indicates HOMOs with high electron density) (c) the LUMOs (where blue indicates LUMOs) and in (d) density of electrostatic potential on the molecular surface (where red indicates negative, blue indicates positive and green indicates neutral)

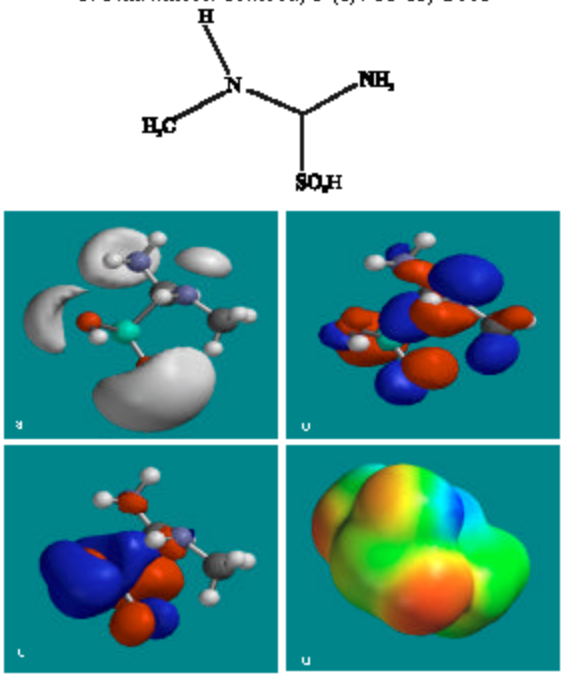

Fig. 10: Structure of MTU-O2H giving in: (a) the electrostatic potential (greyish envelope denotes negative electrostatic potential), (b) the HOMOs, (where red indicates HOMOs with high electron density)(c) the LUMOs (where blue indicates LUMOs) and in (d) density of electrostatic potential on the molecular surface (where red indicates negative, blue indicates positive and green indicates neutral)

The LUMO-HOMO energy differences for MET and its metabolites from DFT calculations are found to range from 4.1 to 6.7 eV, indicating that the compounds would vary in their kinetic lability.

In the case of MET and SHMET, the electrostatic potential is found to be more negative around the nitrogen of the imidazole ring that is involved in C = N bond, indicating that the position may be subject to electrophilic attack. In the case of MTU, the electrostatic potential is found to be more negative around sulfur atom, indicating that the position may be subject to electrophilic attack. In the case of MEH, the electrostatic potential is found to be more negative around oxygen and sulfur atoms, indicating that the positions may be subject to electrophilic attack.

In the case of MET-EPO and MET-DIOL, the electrostatic potential is found to be more negative around oxygen and nitrogen atoms, indicating that the positions may be subject to electrophilic attack. In the case of GLX, the electrostatic potential is found to be more negative around the carbonyl oxygen atoms, indicating that the positions may be subject to electrophilic attack. In the case of MTU-OH and MTU-O2H, the electrostatic potential is found to be more negative around sulfur atom, oxygen and nitrogen atoms, indicating that the positions may be subject to electrophilic attack.

In the case of MET, MET-DIOL and GLX, the HOMOs with high electron density are found to be more widely distributed than the LUMOs. In the case of SHMET, MTU, MEH, MET-EPO, both the HOMOs with high electron density and the LUMOs cover nearly all the non-hydrogen atoms.

The overlap of HOMO with high electron density and region of negative electrostatic potential at some positions, gives further support to the idea that the positions may be subject to electrophilic attack.

The molecular surface of MET and its metabolites SHMET, MTU, MEH, MET-EPO, MTU-DIOL, GLX, MTU-OH and MTUO2H are found to possess negative (yellow and red) and neutral

(green) regions so that they may be subject to electrophilic and lyophilic attacks. The molecular surfaces of MET, MET-EPO and GLX are also found to possess significant amounts of electron-deficient (blue) regions so that they may also be subjected to nucleophilic attacks. Nucleophilic attacks can be due to glutathione and nucleobases in DNA. Reaction with glutathione can induce cellular toxicity by compromising the antioxidant status of the cell whereas that with nucleobases in DNA can cause DNA damage. The rates of such adverse reactions are expected to be appreciable in the case of moderately labile metabolite GLX.

The solvation energy values of MET and its metabolites from PM3 calculations in kcal mol^{-1} are found to range -7.3 to -10.4, indicating that all the compounds would be moderately soluble in water.

CONCLUSION

Methimazole is a tautomeric cyclic thione used to treat various auto-immune diseases such as hyperthyroidism in humans. The molecular surfaces of MET, MTU, MET-EPO and GLX are found to possess significant amounts of electron-deficient (blue) regions so that they can react with cellular nucleophiles such as glutathione and nucleobases in DNA, thus causing depletion of glutathione and oxidation of nucleobases. The former would induce cellular toxicity due to oxidative stress and the latter would cause DNA damage. The rates of such adverse reactions are expected to be significant for GLX which would be moderately labile kinetically. This means that the toxicity due to MET may be mediated via the formation of GLX although the parent drug itself may also be responsible for toxicity if the rates of its reactions with glutathione and nucleobases in DNA are speeded up enzymatically.

ACKNOWLEDGMENTS

Fazlul Huq is grateful to the Discipline of Biomedical Science, School of Medical Sciences, The University of Sydney for the time release from teaching.

Abbreviations

MET: GSH: SHMET: MTU: MEH: MET-EPO: MET-DIOL: GLX: DFT: LUMO: HOMO

REFERENCES

Engler, H., A. Taurog and T. Nakashima, 1982. Mechanism of inactivation of thyroid peroxidase by thioreylene drugs, Biochem. Pharmacol., 31: 3801-3806.

Meng, C.Q., 2006. Inhibitors of the expression of vascular cell adhesion molecule-1. Annual Reports. Med. Chem., 41: 197-210.

Mizutani, M., K. Yoshida, M. Murakami, M. Shirai and S. Kawazoe, 1999. Evidence for the involvement of N-methylthiourea, a ring cleavage metabolite, in the hepatotoxicity of methimazole in glutathione-depleted mice: Structure-toxicity and metabolic studies. Chem. Res. Toxicol., 13: 170-176.

Schiffman, S.S., 1983. Taste and smell in disease. N. Eng. J. Med., 308: 1275-1279.

Schimdt, G., G. Borsch, K.M. Muller and M. Wagener, 1986. Methimazole-associated cholestatic liver injury: Case report and brief literature review. Hepato-gastroenterology, 33: 244-246.

Spartan '02, Wavefunction, Inc. Irvine, CA, USA, 2002.

Vitug, A. and J. Goldman, 1985. Hepatotoxicity from antithyroid drugs. Horm. Res., 21: 229-234.

Wing, S. and I. Fantus, 1987. Adverse immunologic effects of antithyroid drugs. CMAJ., 136: 121-127.